Time Resolved Molecular Beam Characteristic in a Pulsed Supersonic Jet

Wee Kyung Kang, Eun Jeong Kim, Chang Ju Choi, Kwang Woo Jung[a] and Kyung-Hoon Jung*

Center for Molecular Science and Department of Chemistry, Korea Advanced Institute of Science and Technology, Taeduck Science Town, Taejon 305-701, Korea

Received November 23, 1994

A pulsed molecular beam source having short pulse duration (typically 70 μs) and narrow velocity distribution ($\Delta v/v \simeq 8$ % for helium) has been constructed utilizing a commercial fuel injector. Beam characteristics of helium and ammonia seeded in helium expansions are accomplished by the use of an electron impact time-of-flight mass spectrometer. The comparisons between experimental data and theoretical calculations show that the proper beam speed is important to predict the evolution of stream temperature and valve shutter function. The decreasing tendency of pulse duration with increasing cluster size leads to the conclusion that the cluster beam property is described as a function of cluster mass and disinct cluster temperature.

Introduction

Highly expanded free jets of gaseous species have found diverse applications in the study of spectroscopy, chemical dynamics, fluid mechanics, analysis, and surface studies.[1~3] The low collision energies in the medium provide a unique environment for the formation of weakly bound molecular complexes. The combined effects of resulting low internal energies and the narrow velocity distribution lead to simple and highly resolvable spectra which aid considerably in elucidating the structure and dynamics of these molecules.[4~8]

Until recently, however, the use of supersonic molecular beams has been limited by the cost and complexity of the required vacuum systems. In addition, the maximum achievable density of a continuous molecular beam has been kept relatively low since it is also limited by the pumping capability of vacuum system. The use of a pulsed molecular beam source can overcome the above limitations to a large extent and the physical dimensions of the source of the molecular beam can be reduced. This reductin of system complexity makes the pulsed valve approach to beam production quite attractive.

The pulsed nozzles for supersonic expansions are now well established and various designs are also available to meet specific requirements. Since late 1970s the current-loop actuated sources have been developed by several research groups[9,10] using the concept of repulsion of two conductors with current flowing in opposite directions. Unfortunately this design requires very large current pulses (thousands of amperes) and high voltages (~2 KV) to drive the valve. Although the short pulsed valve (10-300 μs) can be constructed, its mechanical and electrical complexities have limited its usefulness when the fast repetition rate and simple construction are required. A piezoelectric devcice[11] was demonstrated to offer high repetition rates (>100 Hz), however, it cannot be used at elevated temperatures and requires periodic replacement of the crystal.

The frequently used pulsed beam source for spectroscopy experiments, where the short pulse duration is less critical as in scattering experiments, has been the solenoid valves. Of the various solenoid valves adapted for molecular beam source, the most popular one is the relatively inexpensive automobile fuel injector.[12,13] Its strong points are comparatively simple to construct with only moderate drive circuitry and operable at high repetition rates (>50 Hz). Unfortunately, however, the gas pulse is typically several hundred microseconds to several milliseconds long. Bassi and co-workers [14] have overcome this limitation using the background interference to reduce the width of the beam pulse while the pumping load at the source region is severe ($>10^{-3}$ Torr).

Aside from the significant improvements in pulsed beam source, very little is known concerning the seeded beam characteristics: the variation of mean velocity and the temperatures of higher clusters in supersonic expansions. This is due partly to the measuring difficulties of individual cluster properties in molecular beam and due partly to the insufficient knowledge of describing the pulsed free jet expansion.

In this laboratory we have found that a fuel injector valve can be used satisfactorily to reduce the pumping demands of the system in an electron impact ionization time-of-flight mass spectrometry (TOFMS)[15] In this paper we describe a relatively simple design of pulsed supersonic beam source in detail, incorporating a fuel injector valve, which produces very short gas pulse (typically 70 μs FWHM for He beam). Time resolution study of the pulsed beam is able to characterize the stream temperature and valve shutter function quantitatively. The beam source is very simple and easy to construct and provides a unique characteristics compared with the more complicated valves in their designs. We have also compared our experimental measurements for the temporal behaviors of the single component and seeded beams with theoretical predictions.

System Design

The experimental apparatus is schematically shown in Fig-

*Author to whom correspondence should be addressed.
[a]Present address: Department of Chemistry, Wonkwang University, Iri 570-749, Korea

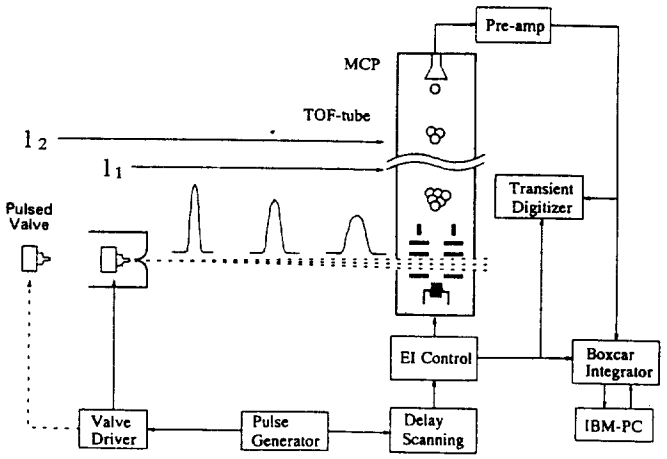

Figure 1. Schematic diagram of the pulsed-molecular beam profile measuring system.

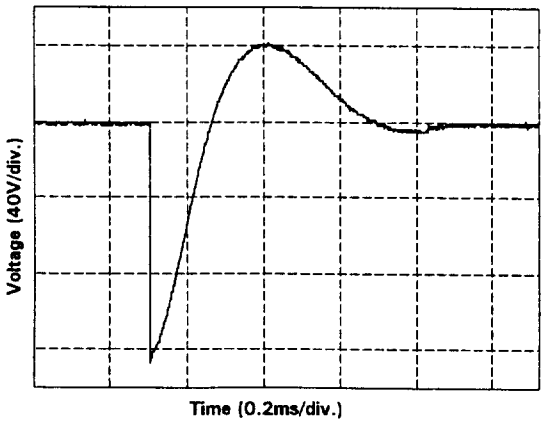

Figure 2. Oscilloscope trace of injector pulse waveform. Vertical scale: 40 V/div., horizontal scale: 200 μs/div.

ure 1. It consists of a differentially pumped vacuum system with a TOFMS sitting vertically on top of the main chamber. The molecular beam is introduced through a pulsed valve in the source chamber, which is pumped by a 4 in. diffusion pump (760 L/s) fitted with a water cooled baffle.

The valve we have used is an automobile fuel injector (Siemens, part No. 9611606076) designed to open for 1-10 ms, at repetition rates up to 50 Hz. It is a solenoid plunger design, wherein a current pulse energizes the solenoid coil, which in turn retracts a metal piston. The external dimensions of the valve were machined down somewhat to facilitate the suitable mounting and gas supply while the nozzle geometry (throat diameter=500 μm) of injector was maintained without any modification. The source chamber is separated from the main chamber by a Cu electroformed conical skimmer with an orifice diameter of 0.8 mm. The nozzle to skimmer distance is 5 mm. The free jet is skimmed and passes through the main chamber which is evacuated by a liquid nitrogen trapped 8 in. diffusion pump (2000 L/s). The source and main chambers are maintained their base pressures below 5×10^{-4} and 2×10^{-6} Torr, respectively, at 10-Hz repetition rate and 5 atm stagnation pressure of He.

A simple capacitor discharge circuit[16] is used to operate the injector. A pulse charging power supply is used to charge a 2 μF capacitor to voltages up to 200 V. A silicon controlled rectifier (SCR) is used to discharge the capacitor and allows a high peak current pulse to flow through the conductors of the pulsed valve. A diode is included in the front end of the circuit to prevent the capacitor from seeing damaging reverse voltage swings. Typical operating conditions are: driving voltage between 120-150 V and electric pulse duration greater than 100 μs (57 A peak current for a 130 V charging voltage). Figure 2 shows the oscilloscope trace of the injector current pulse. The driver circuit is usually operated at 10 Hz although operation at higher repetition rate produces no noticeable change in the gas pulse characteristics.

Beam analysis is performed by means of an electron impact TOFMS,[15] placed at a 10 cm from the source. After a delay time with respect to the timing of the injector trigger pulse, the molecular beam is ionized by applying the electron impact pulse at orthogonal direction. The ions are modulated by pulsing of the voltage of the first extraction lens of the ion source. The pulsing of ions is used as the reference signal for the time-of flight measurements using the conventional method. The arrival time distribution of the ion packet is measured with time resolution of 10 ns by using a transient digitizer and signal averager (LeCroy, Model 9400A). The ions are detected by a chevron microchannel plate (MCP) detector. The drift tube is differentially pumped by a turbomolecular pump with effective pumping capacity of 200 L/s. The base pressure in the drift region, typically 1×10^{-7} Torr, rises to about 5×10^{-7} Torr during operation. For the pulse width measurements of molecular beam the MCP output is sent to a boxcar averager (Stanford Research Systems) gated at the appropriate arrival time of interesting ion. After averaging, the results are stored in a microcomputer.

Molecular Beam Characterization

Pulsed Nozzle Performance. In order to determine the temporal distribution and beam characteristics of a pulsed molecular beam emerging from the valve, we probed the beam with TOFMS technique. The electron impact pulse was delayed by varying delay time ranging from zero to 1 ms after the valve circuit began to open the nozzle. An example of molecular beam signals taken for 5 atm He expansion with different values of nozzle-detector distance is shown in Figure 3. Helium was chosen because its use as a seed gas makes it a common constituent of the molecular beam produced in our system. The pulsed beam sources are situated at $l_1=11.1$ cm and $l_2=44.1$ cm in the ionization region of mass spectrometer. This measurement was performed without skimmer and operated under typical driver condition (10 Hz). The peak intensities of two signals were normalized to facilitate comparisons between them. Time zero in the figure corresponds to triggering of the pulsed valve. One can immediately notice that the measured pulse widths of the molecular beam are very close to that of the current pulse applied to the injector.

From the measured time difference between two positions, the mean speed (stream velocity, v_s, of the molecular beam) of He atoms is estimated to be 1.38×10^5 cm/s. The most

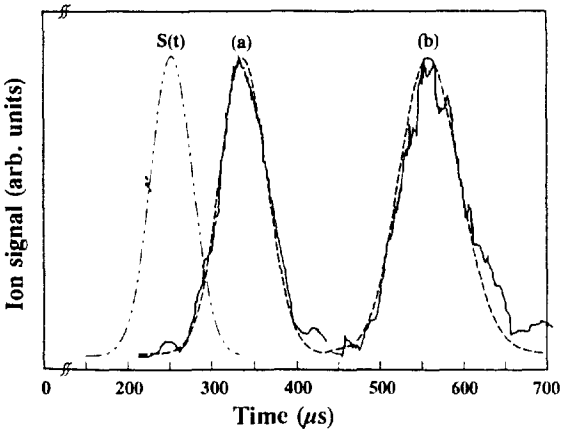

Figure 3. Typical beam pulse at distances (a) $l_1=11.1$ cm and (b) $l_2=44.1$ cm from the ionization region of TOFMS. $S(t)$ is the calculated valve shutter function. The calculated detector responses (dashed lines), employing by Eq. (3) with $v_s=1.38\times10^5$ cm s^{-1}, show a good agreement with the experimental observations (solid lines). $t=0$ is the trigger point for the pulsed valve. The gas used was helium at an inlet pressure to the pulsed valve of 5 atm.

probable velocity in the molecular beam, v_p, is well characterized by $\alpha(3/2)^{1/2}$ instead of α as found for molecules in the effective source:[17]

$$\alpha=(2kT/m)^{1/2} \tag{1}$$

where k is the Boltzmann constant, T is the source temperature, and m is the mass of the molecule. Thus, for a supersonic beam of He the most probable velocity at 300 K is predicted to be $v_p=1.37\times10^5$ cm/s, in accurate accord with experiment.

It has been known that the mean velocity rises quickly and asymptotically approaches the terminal velocity,[18] v_t. That is, the velocity reaches 98% of v_t within a few diameters ($x/d\sim5$ for monoatomic gases). This feature is very important in understanding the valve opening time. Therefore, the actual flight time t_1 of molecular beam from the l_1 position to the detector is only 80 μs. The time corresponding to the peak signal, however, is 330 μs, indicating a delay of about 250 μs between the trigger pulse and the time of maximum valve opening. The delay is the time required to set the metal piston in motion and accelerate the gas pulse out of the nozzle. The pulse widths measured at the l_1 and l_2 points are $\tau(l_1)=70.1$ and $\tau(l_2)=74.6$ μs FWHM, respectively. It should be noted here that the measured width of the gas pulse in these experiments is due not only to the valve shutter time but also to the beam velocity distribution at the ionizing point.

The observed spread in arrival times at each distance can be expressed by the convolution of the opening time of the valve, τ_s, and the spread, τ_v, due to the velocity distribution in the beam. We assume these contributions combine, like the convolution of two Gaussian distributions, to give the total time spread, τ_{tot}, at the detector by,

$$\tau_{tot}^2=\tau_s^2+\tau_v^2. \tag{2}$$

If the velocity distribution does not contribute to $\tau(l_1)$, as Gentry and Giese[9] suggested, we may take $\tau_s\simeq\tau(l_1)$. For the He beam (Figure 3) the velocity spread, $\Delta v/v$ ($\simeq\tau_v/t_2$), is then approximately 8% for the valve opening time $\tau_s=70.1$ μs. The present experiments clearly demonstrate that the expansion from a nozzle source into high vacuum results in adiabatic cooling of the molecular flow. This cooling is a real reduction in Maxwell velocity distribution relative to the center of mass flow velocity. The comparison of data taken at different nozzle-detector distance shows that the velocity distribution of the beam is very narrow and that the pulse width is determined mainly by the valve opening time.

In order to understand more fully the valve shutter function, $S(t)$, and the stream temperature, T_s, of the molecular beam, we employed, using the conventional supersonic beam theory,[19] a mathematical model that relates the time dependence of the detector signal to a time- and velocity-dependent flux from the pulsed valve. The function $S(t)$ represents the temporal action of the pulsed valve in releasing a burst of gas toward the ionization region of TOFMS. The detector signal $D(t)$ is given by the convolution between the $S(t)$ and the molecular beam velocity distribution $f(v)$. Let us assume that each segment so sampled has a Maxwell velocity distribution with stream temperature T_s and stream velocity v_s, and that these quantities do not change significantly during the valve opening time. The detector response $D(t)$, converted to a time distribution using Jacobian transformation, to the pulse produced by the valve is mathematically expressed by,

$$D(t)\propto\int_0^t S(t')\frac{l^3}{(t-t')^4}\exp\left[-\left(\frac{m}{2kT_s}\right)\left(\frac{l}{t-t'}-v_s\right)^2\right]dt', \tag{3}$$

where l is the distance between the valve and the ionizing point of mass spectrometer. Equation (3) takes into account the velocity dependence of the detection efficiency by multiplying v^{-1} to the velocity distribution. With the experimentally obtained v_2 value, the above equation contains only two parameters: the stream temperature T_s, which is related to the Mach number of the molecular beam, and the shutter function S(t). As shown in Figure 3, there are good agreements between the measured and calculated temporal behaviors of molecular beams. The present result shows that the inclusion of the proper beam speed is important to predict the evolution of stream temperature and valve shutter function. The calculated values of $T_s=7$ K and $S(t)=63.6$ μs are obtained from the above simulation. It should be pointed out that simply assuming no contribution of velocity distribution to $\tau(l_1)$, as mentioned above, results in overestimation of $S(t)$ function by 9%. Mach number, M_s, for gas stream then can easily be calculated by,

$$M_s=\frac{v_s}{(\gamma kT_s/m)^{1/2}}, \tag{4}$$

where γ is the specific heat ratio. For a supersonic beam of He, Mach number is determined to be $M_s\simeq9$.

The discrepancy between the theoretical expression and the experimental points at the wings of the distribution may well be due to the asymmetric shape of the original gas pulse and a contribution from the incomplete supersonic ex-

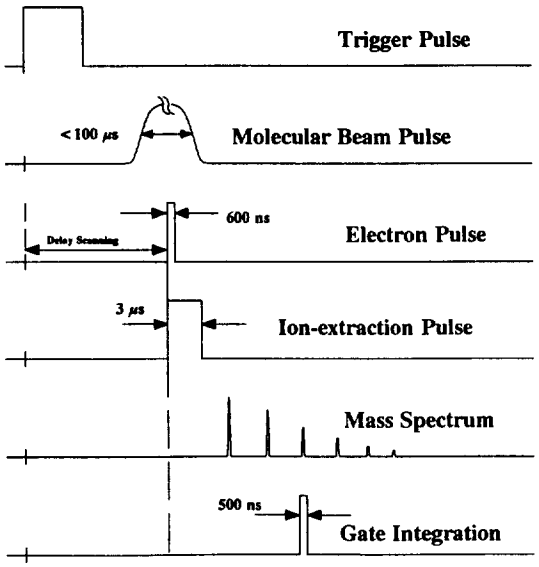

Figure 4. Pulsed sequence used to measure the beam pulse width of each cluster in the molecular beam.

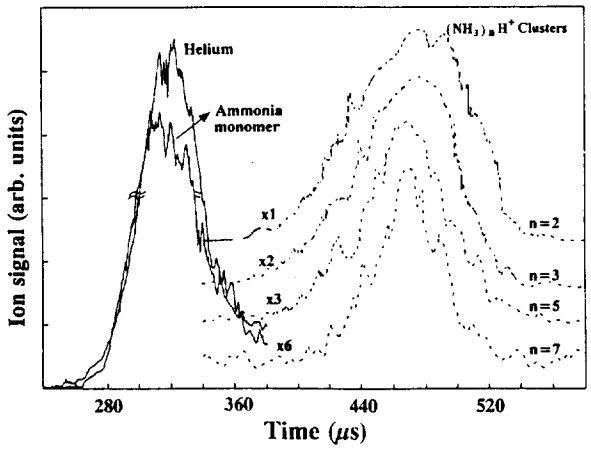

Figure 5. Temporal profiles of various ammonia cluster beams as a function of the delay between opening the molecular beam valve and pulsing the electron beam. The peak intensities of the cluster signals have been normalized to facilitate comparisons between them. The molecular beam is expanded with 3% ammonia seeded in 5 atm He.

pansion at the pulse beginning and end. Saenger and co-workers[20] have shown that the minimum safe pulse width to ensure complete supersonic expansions is of order of 10 μs. The present pulse width is sufficiently long to satisfy the above condition at the gas pulse center and short enough to keep the gas load to a minimum. For a pulsed valve operated with 5 atm pressure in the source, the pulsed beam flux at the ionization region is estimated to be more than 10^{20} atoms $sr^{-1}s^{-1}$ for He (see Appendix).

Cluster Beam Characterization. Supersonic expansions provide unique environments to study the spectroscopy and dynamics of cold gas-phase molecules. They are also efficient sources of weakly bound clusters in elucidating the intracluster ion-molecule reactions and the structures of clusters.[21,22] However, the distribution of cluster species formed in these expansions can make it very difficult to measure properties of a monomer or of a particular size cluster. Pulsed molecular beams, where the cluster distribution depends strongly on time within the pulse, are still more complicated. Further information on the beam properties of clusters inside pulsed molecular beams comes from measuring the intensity of different cluster ions as a function of time within the beam pulse.

The electron impact ionization combined with TOF mass spectrometry is a useful method for assessing the property of cluster beam. Figure 4 illustrates typical timing parameters for the synchronization of the injector trigger signal, the electron impact pulse, the ion detection, and the gate integration during the pulse width measurements of various clusters in the molecular beam. Triggering the molecular beam valve starts the pulse sequence. After a delay to allow the sample molecules to reach the ionizer, a positive-going pulse coupled onto the electron-extractor electrode initiates the electron pulse. Following a short delay, a positive pulse coupled onto the ion-extraction electrode accelerates the resulting ions into the ion drift region. We choose the amplitude of this pulse to satisfy the space-focusing condition, and its duration is sufficient to ensure that all of the ions have entered the drift region before the pulse ends. In this application, the temporal behavior of the ion signal in the detector of mass spectrometer reflects the evolution of the gas density in the ionization region, permitting accurate measurement of the temporal profiles of the each clusters.

Figure 5 displays the temporal distributions of various $(NH_3)_nH^+$ clusters within a molecular beam of 3% NH_3 seeded in 5 atm helium. The experiments were performed at a nozzle-ionization distance of 11.1 cm with skimmer. An interesting feature is observed; the molecular beam is classified into two groups having different velocity components. The fast beam component corresponds to the helium and ammonia monomer ion while the slow component consists of only ammonia clusters. This result indicates that the inherent pulsed nature of the gas flow has a profound effect on the cluster beam characteristics. So far, it has been known that if the mixture gas consists of a small fraction of smaple molecule (such as NH_3 in this study) seeded in an excess of light carrier gas, the seed molecules will be accelerated to a speed, very nearly, equal to that of the carrier molecules. The exact accordance of monomer ion signal with the temporal profile of He carrier gas suggests the validity of conventional concepts. It is quite surprising, however, that the velocity of cluster beam is slower than the helium and ammonia monomer beam. This velocity slip can be explained by the fact that a noncontinuum, translational relaxation effect[23] between species within molecular beam occurs in the subsonic region of the nozzle, resulting in the variation of the mean velocities. The effective cluster formation during the initial acceleration stage in supersonic expansion provokes the distinct molecular beam property which can be separated into two components, *e.g.*, low mass (helium and ammonia monomers) and high mass (ammonia clusters) beams.

Another distinct feature to be noted is that the pulse widths of clusters show a decreasing tendency with increasing cluster size. Although the cluster ion distribution, in general, do not relfect the explicit distribution of the neutral clusters, it provides a qualitative identification of the cluster property.

Table 1. Calculated stream temperatures of ammonia clusters[a]

Cluster size, $(NH_3)_nH^+$	2	3	5	7
Measured pulse width (μs)	85.9	68.5	61.7	54.8
Stream temperature, T_s (K)	85	45	25	3

[a] Data fitting has been optimized for v_s=730 m/s and $S(t)$=63.6 μs.

For example, neutral ammonia clusters greater than the tetramer $(NH_3)_4$ can contribute to the temporal profile of $(NH_3)_3H^+$ cluster ion (see Figure 5) through intracluster protonation reaction and evaporation mechanism,[24] whereas neutral trimer cannot. This unprecedented observation of temporal behavior of the clusters cannot be explained by a simple kinetic theory. One of the possible rationales of our result is that for the same v_s and T_s the lighter species will have a larger velocity component in a direction perpendicular to the molecular beam axis, causing more lateral spreading. This means that the mass of the molecule, m, in Maxwell velocity distribution function gives a contribution to the temporal broadening of the molecular beam. When we tried to simulate the cluster beam profiles with the detector response $D(t)$ function, as described above, there was a significant discrepancy between the calculated waveforms and the actual data, indicating that another factor plays an important role to the cluster beam characteristics.

Anomalous behavior of cluster beam can be explained partly by cooling effects of cluster temperatures. The cluster temperatures obtained from our data fitting are listed in Table 1. The stream temperature of cluster beam steeply decreases with increasing cluster size. This is suggestive of the fact that the clustering of the gas molecules is an another factor affecting the beam property. The cooling of clusters produced in supersonic beams can proceed by two microscopically distinct mechanisms. The first is collisional cooling, that is the relaxation of internal degrees of freedom by two-body collisions to the monomers and/or the carrier gas. The second mechanism is evaporative cooling, that is, unimolecular dissociation of large metastable clusters, which proceeds throughout the time of transit up to the ionizing point, even after collisional cooling has ceased.

Conclusions

In this paper we have described the construction and performance of a versatile, simple molecular beam source and demonstrated that this can be successfully used to produce short and intense molecular beam pulses. The generalized Maxwell equation has been used to investigate quantitatively the evolution of the stream temperatures, valve shutter function, and the unexpected beam characteristics in a supersonic expansion of a single component and seeded beam. The design and characteristics of this reliable, 10 Hz repetition rate pulsed molecular beam source should encourage the use of pulsed, supersonic molecular beams in an increasing number of applications. We are currently employing this design in our laboratory to study intracluster ion-molecule reaction and photofragment spectroscopy.

Acknowledgment. This work was carried out with financial assistance from the Korea Science & Engineering Foundation, which is gratefully acknowledged.

Appendix: Estimation of Beam Flux

The beam flux F, can be estimated approximately from the beam profile using an equation derived from the free jet expansion. The throughput Q (defined as the quantity of gas flowing through a hole) of gas expanding from the orifice of a supersonic valve can be related to source conditions[23] by

$$Q=C(T_c/T_0)\sqrt{300/T_0}(P_0d^2) \quad \text{(A1)}$$

where C is a constant, T_c is the vacuum chamber temperature usually assumed to be at room temperature, T_0 is the stagnation temperature, P_0 is the stagnation pressure, and d is the diameter of the nozzle. The use of a pulsed valve can reduce Q_p considerably provided the duty cycle is small. The duty cycle is given by $\tau_p\nu$ where τ_p is the pulse duration and ν the repetition rate. Q_p is then given by,

$$Q_p=C(T_c/T_0)\sqrt{300/T_0}(P_0d^2)\tau_p\nu \quad \text{(A2)}$$

Using typical values for He (C=45 $km^{-2}s^{-1}$, T_0=300 K, P_0=5 atm, d=0.05 cm, τ_p=100 μs FWHM, and ν=1 Hz), we obtain a pulse throughput of $Q_p\simeq1.4\times10^{18}$ atoms s^{-1}.

In the differentially pumped two chamber MB/EI/TOFMS system, only a small central portion of the expanding gas is allowed to enter through a skimmer to the second (main) chamber where excitation and detection occur. The beam flux, F_d, through the ionization volume of detector is calculated by,

$$F_d=Q_p/\Omega \quad \text{(A3)}$$

where the solid angle Ω is given by,

$$\Omega=A/L^2 \quad \text{(A4)}$$

In the equation A and L represent the area of the focal volume cross section ($\simeq$19.6 mm^2) and the nozzle to ionization distance (11.1 cm), respectively. Therefore, the flux density is calculated to be 8.7×10^{20} atoms $sr^{-1}s^{-1}$.

References

1. Anderson, J. B. *Molecular Beams and Low Density Gasdynamics*; Weggner, P. P., Ed.; Dekker: New York, U. S. A., 1974; p 1.
2. Hagena, O. F. *Surf. Sci.* **1981**, *106*, 101.
3. Gentry, W. R. *Atomic and Molecular Beam Methods*; Scoles, G. Ed.; Oxford University Press: New York, U. S. A., 1988; p 54.
4. Smalley, R. E.; Levy, D. H.; Wharton, L. *J. Chem. Phys.* **1976**, *64*, 3266.
5. Smalley, R. E.; Wharton, L.; Levy, D. H.; Chandler, D. W. *J. Chem. Phys.* **1978**, *68*, 2472.
6. Lovejoy, C. M.; Nesbitt, D. J. *Rev. Sci. Instrum.* **1987**, *58*, 807.
7. Castleman, Jr. A. W.; Keesee, R. G. *Chem. Rev.* **1986**, *86*, 589.

8. Balle, T. J.; Flygare, W. H. *Rev. Sci. Instrum.* **1981**, *52*, 33.
9. Gentry, W. R.; Giese, C. F. *Rev. Sci. Instrum.* **1978**, *49*, 595.
10. Liverman, M. G.; Beck, S. M.; Monts, D. L.; Smalley, R. E. *J. Chem. Phys.* **1979**, *70*, 192.
11. Auerbach, A.; McDiarmid, R. *Rev. Sci. Instrum.* **1980**, *51*, 1273.
12. Behlen, F. M.; Rice, S. A. *J. Chem. Phys.* **1981**, *75*, 5672.
13. Shinohara, H. *J. Chem. Phys.* **1983**, *79*, 1732.
14. Bassi, D.; Iannotta, S.; Niccolini, S. *Rev. Sci. Instrum.* **1981**, *52*, 8.
15. Jung, K. W.; Choi, S. S.; Jung, K.-H. *Rev. Sci. Instrum.* **1991**, *62*, 2125.
16. Otis, C. E.; Johnson, P. M. *Rev. Sci. Instrum.* **1980**, *51*, 1128.
17. Ramsey, N. F. *Molecular Beams*; Oxford University: New York, U. S. A., 1990; p 11.
18. Scoles, G. *Atomic and Molecular Beam Methods*; Oxford University: New York, U. S. A., 1988; p 3.
19. Anderson, J. B.; Hagena, O. F. *Molecular Beams and Low Density Gasdynamics*; Wegener, P. P. Ed.; Dekker: New York, U. S. A., 1979.
20. Saenger, K. L.; Fenn, J. B. *J. Chem. Phys.* **1983**, *79*, 6043.
21. Jung, K. W.; Choi, S. S.; Jung, K.-H. *Bull. Korean Chem. Soc.* **1992**, *13*, 306.
22. Shin, D. N.; Jung, K. W.; Jung, K.-H. *J. Am. Chem. Soc.* **1992**, *114*, 6926.
23. Miller, D. R. *Atomic and Molecular Beam Methods*; Scoles, G. Ed.; Oxford University: New York, U. S. A., 1988; p 14.
24. Shinohara, H.; Nishi, N; Washida, N. *Chem. Phys. Lett.* **1988**, *153*, 417.

Single Crystal EPR Spectra of $K_{12}[As_2W_{18}O_{66}Cu_3(H_2O)_2]\cdot 11H_2O$, a Copper(II) Trimer

Young Hwan Cho and Hyunsoo So*

Department of Chemistry, Sogang University, Seoul 121-742, Korea
Received November 24, 1994

Single crystal EPR spectra of $K_{12}[As_2W_{18}O_{66}Cu_3(H_2O)_2]\cdot 11H_2O$ exhibit an orientation-dependent fine structure of an $S=3/2$ system which is accounted for by the exchange and magnetic dipole interactions among the three Cu^{2+} ions. The hyperfine structure and the lines from the $S=1/2$ manifolds have not been observed. The isotropic exchange parameters determined from the magnetic susceptibility data at 5-300 K are $J_1=J_2=-7.8$ cm^{-1}. The magnitude of J values suggests that the unpaired electrons on three Cu^{2+} ions interact through a sequence of six bonds involving two tungsten atoms and three oxygen atoms. The Cu-Cu distance, 4.37 Å, determined from the EPR spectra is considerably smaller than the value from the X-ray crystal structure determination, 4.76± 0.03 Å, indicating that the point-dipole model underestimates the dipolar interaction.

Introduction

Although EPR spectra of monomeric transition metal complexes are well understood, a detailed description of the EPR spectra for oligomeric metal ion clusters is still in a developing stage. The EPR spectrum of the binuclear copper(II) acetate, first studied by Bleaney and Bowers in 1952,[1] has revealed that both exchange and dipole-dipole interactions are important for this complex, in which the Cu-Cu separation is 2.6 Å. When the metal-metal separation is large and the exchange interaction is small, the metal separation may be determined from the dipolar splitting in the EPR spectra.[2] This technique has been used to deduce the metal ion separations for a number of dimers of copper(II), oxovanadium (IV), and titanium(III) which have unknown structure. The accuracy of the metal separations determined by this technique has not been tested with sufficient number of compounds whose structures are known. In addition, when the principal axes of the two metal ions are not parallel, a perturbation expression can be derived only for zero exchange interaction.[2] Recently we have found that both analysis of the EPR spectra and determination of the metal separation are not very reliable, if a small exchange interaction is neglected for this type of compound.[14]

As the number of paramagnetic transition metal ions increases, the EPR spectrum gets more complicated. In order to understand their EPR spectra, we need to study compounds with known structures. Some polyoxometalates were suggested as good systems for studying magnetic interactions among the metal ions, and some powder EPR spectra have been reported.[6] We have been studying single crystal EPR spectra of some polyoxometalates containing more than one paramagnetic transition metal ion. This paper reports the single crystal EPR spectra of a copper trimer, $[As_2W_{18}O_{66}Cu_3(H_2O)_2]^{12-}$ (hereafter denoted as As_2Cu_3). The X-ray crystal structure of this anion (Figure 1) shows three Cu(II) ions sandwiched between two AsW_9O_{33} subunits.[4] There are two types of copper ions, arranged in an isosceles triangle; Cu(1) is in a square planar environment and Cu(2) and Cu(3), related by a mirror plane, are in square pyramidal environments.